A Letters Journal Exploring the Frontiers of Physics

January 2008

EPL, **81** (2008) 17005
doi: 10.1209/0295-5075/81/17005

www.epljournal.org

Magnetic coupling in highly ordered NiO/Fe_3O_4(110): Ultrasharp magnetic interfaces vs. long-range magnetoelastic interactions

I. P. Krug[1(a)], F. U. Hillebrecht[1†], H. Gomonaj[2], M. W. Haverkort[2], A. Tanaka[3], L. H. Tjeng[4] and C. M. Schneider[1]

[1] *Institut für Festkörperforschung IFF-9, Forschungszentrum Jülich GmbH - 52425 Jülich, Germany*
[2] *Bogolyubov Institute for Theoretical Physics NAS of Ukraine - st. Metrologichna, 14-b, 03143, Kiev, Ukraine*
[3] *Department of Quantum Matter, ADSM, Hiroshima University - Higashi-Hiroshima, 739-8530, Japan*
[4] *Physikalisches Institut II, Universität zu Köln - 50937 Köln, Germany*

received 22 August 2007; accepted 28 October 2007
published online 20 November 2007

PACS 75.70.Cn – Magnetic properties of interfaces (multilayers, superlattices, heterostructures)
PACS 75.70.Ak – Magnetic properties of monolayers and thin films
PACS 75.25.+z – Spin arrangements in magnetically ordered materials (including neutron and spin-polarized electron studies, synchrotron-source X-ray scattering, etc.)

Abstract – We present a laterally resolved X-ray magnetic dichroism study of the magnetic proximity effect in a highly ordered oxide system, *i.e.* NiO films on Fe_3O_4(110). We found that the magnetic interface shows an ultrasharp electronic, magnetic and structural transition from the ferrimagnet to the antiferromagnet. The monolayer which forms the interface reconstructs to $NiFe_2O_4$ and exhibits an enhanced Fe and Ni orbital moment, possibly caused by bonding anisotropy or electronic interaction between Fe and Ni cations. The absence of spin-flop coupling for this crystallographic orientation can be explained by a structurally uncompensated interface and additional magnetoelastic effects.

Introduction. – Many of today's spintronics devices make extensive use of magnetic coupling phenomena, in particular, through non-magnetic interlayers or between antiferromagnetic (AF) and ferr(o/i)magnetic (henceforth labeled F(I)M) constituents. The latter coupling is well known to give rise to the so-called exchange anisotropy or "exchange bias" [1]. In spite of huge scientific efforts in this field, the relation between the exchange biasing phenomenon and the microscopic spin configurations in both constituents and across the interface is still a matter of debate. In addition, a detailed experimental insight into these magnetic proximity effects is often compromised by the imperfection of the interface and the unknown role of defects. A key factor in discriminating different magnetic coupling mechanisms and elucidating their physical origin is the crystalline and chemical perfection of the sample. In order to unequivocally address the details of the spin-dependent coupling mechanisms, highly ordered systems with well-defined interface roughness and good crystallinity are mandatory. This gives also a chance to make better contact to the various theoretical models.

Mean-field calculations have shown that in case of an ideal crystalline system with only nearest-neighbor interactions, the interaction zone can be extremely narrow, in the order of a few monolayers on either side of the interface [2]. Even an atomically sharp transition is possible, as has been found experimentally for highly ordered MnPt/Fe systems [3]. The magnetic structure of this *planar domain wall* plays a key role for exchange bias, since it determines whether or not Zeeman energy can be stored reversibly, if an external field is applied (so-called exchange spring) [4]. An important source of the magnetic proximity effect is the variation of the size and relative orientation of the spin and orbital moments in the vicinity of the interface, caused by electronic interaction of the two layers in contact [5,6]. Even violations of Hund's third rule were predicted, *i.e.* the mutual orientation of spin and orbital moment is not dominated by the filling of the bands carrying the magnetic moment, but rather by ligand

(a) E-mail: i.krug@fz-juelich.de
† Deceased.

field and hybridization effects [5,6]. Another remarkable feature in this context is the prediction of a reversal of the uncompensated magnetization in the antiferromagnet from one interfacial layer to the next, which is induced by the interplay of the unidirectional interface anisotropy and the antiparallel coupling of neighboring atoms within the antiferromagnet [2,7].

In this contribution, we report the observation of a pronounced proximity effect in thin NiO films grown on ferrimagnetic $Fe_3O_4(110)$ single crystals. We find strong evidence for an atomically sharp electronic, magnetic and structural transition with a collinear coupling between the AF and FIM. The details of the coupling show no evidence of a sign reversal in the uncompensated magnetization for successive interfacial monolayers in the antiferromagnet. Already the second monolayer appears to be fully spin-compensated, with vanishing spin and orbital moment.

Experimental details. – Our choice of $NiO/Fe_3O_4(110)$ represents an almost ideal model system, since the small lattice mismatch (0.5%) results in pseudomorphic growth and sharp interfaces [8,9]. Contrary to metal/oxide interfaces, which are often diffuse due to chemical interface reactions [10,11], the density of defect spins in a purely oxidic system is generally thought to be very low. In a highly ordered crystalline system we can thus expect to find well-defined magnetic interfaces. We use soft X-ray photoelectron emission microscopy (PEEM) to arrive at an element-sensitive and spatially resolved vectorial magnetometry of the individual FIM and AF constituents by exploiting circular (XMCD) and linear magnetic dichroism (XMLD), respectively.

The measurements were carried out at the BESSY UE-56/1 SGM beamline using an Elmitec PEEM III (resolution $< 100\,\mathrm{nm}$), equipped with an *in situ* preparation facility. The incidence angle to the surface was fixed to 16°, with a degree of circular (linear) X-ray polarization of typically $> 90\%$. The photon energy resolution was set to $< 0.2\,\mathrm{eV}$. Our substrates were synthetic magnetite single crystals, sputter-cleaned with 1 keV Ar ions and subsequently annealed in $10^{-6}\,\mathrm{mbar}$ O_2 at 1100 K for several hours. After verifying the Fe_3O_4 phase by X-ray absorption spectroscopy (XAS) and XMCD, NiO was deposited by molecular beam epitaxy under normal incidence in $10^{-6}\,\mathrm{mbar}$ O_2 background pressure at 300 K ($p_{\mathrm{base}} < 2 \cdot 10^{-9}\,\mathrm{mbar}$). The low deposition temperature was chosen on purpose to avoid thermal intermixing at the interface. Wang *et al.* have shown that in such films the electronic transition from Fe_3O_4 to NiO at the interface is nearly atomically sharp [9].

Closure domain structure of $Fe_3O_4(110)$. – Figure 1 shows a typical domain pattern of the (110)-oriented Fe_3O_4 substrate measured by XMCD at the Fe L_3 edge. Since two of the easy axes of magnetite are coplanar with the (110)-interface, the resulting surface closure domains will consist of two sets of 180° domains, each belonging to an easy axis [12]. As can be seen in fig. 1B,

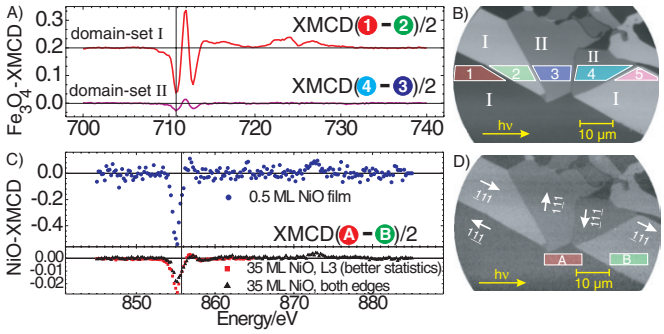

Fig. 1: (Color online) A) Fe_3O_4-XMCD microspectra. Vertical line: energy position for the ratio image. B) Fe_3O_4: ratio image σ^+/σ^-. The numbers 1–5 represent areas of interest (AOI) for the microspectra. Latin numbers were assigned to classify domains by their easy axes: $[\underline{1}11] \rightarrow$ (I) and $[1\underline{1}1] \rightarrow$ (II). C) NiO: XMCD microspectra for a 0.5 and 35 ML NiO film. Vertical line: energy position for the ratio image. D) NiO: XMCD ratio image and magnetization map derived from the spectra (white arrows: Fe_3O_4 and NiO net magnetization).

the stronger contrast levels (black, white) belong to the $[\underline{1}11]$-direction and are labelled Set I. The intermediate gray levels belong to magnetization directions almost perpendicular to the (horizontal) light incidence direction, and can thus be attributed to the $[1\underline{1}1]$-direction (Set II). A quantitative comparison of the XMCD contrast in both sets from the spectra in A) yields an angle of $109 \pm 1°$ between both easy axes, which is close to twice the theoretically expected "magic" angle of 54.73°. As verified from the XMCD contrast and Laue diffraction measurements, the straight domain boundaries run along $\langle 111 \rangle$-type directions as well. Thus, we conclude that the magnetization inside the domains indeed points along the in-plane easy axes. We also performed XMCD measurements at the Ni L_3 edge, which yield information about the uncompensated magnetization in the AF. The contrast levels in fig. 1D are identical to fig. 1B, *i.e.* the Ni moment is parallel to the Fe moment. We will discuss this in more detail in a later section.

Spin axis orientation of the antiferromagnet. – To see how the antiferromagnetic part of the film couples to the Fe_3O_4 surface, we determined the orientation of the spin axis in NiO exploiting the linear dichroism at the L_2 edge. The absence of a shift of the NiO L_3 peak position between p- and s-polarization clearly proves the crystal field dichroism to be negligible [13]. Temperature-dependent XMLD measurements performed after our experiment verified a lowered blocking temperature around 480 K due to finite-size effects [14]. Thus, we conclude that the observed contrast is of purely magnetic origin.

The experimental approach that we have chosen is similar to the one in refs. [14–16], where the ratio of the multiplet-split NiO L_2 peaks was evaluated. However, since with our epitaxial NiO films we have

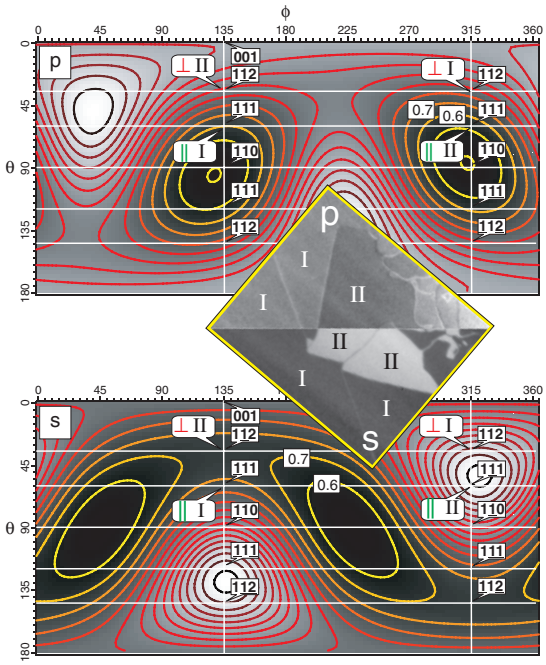

Fig. 2: (Color online) 35 ML NiO on Fe_3O_4(110). The contour plots show the calculated L_2 asymmetry for every possible direction of the spin (angles θ, ϕ). Center: compilation image of PEEM p-contrast (upper half) and s-contrast (lower half). The two domain sets (gray levels) are named I and II. In the contour plots, the corresponding crystallographic directions are labelled. Collinear coupling: [$\underline{1}$11] for set I and [11$\underline{1}$] for set II. Conversely for spin-flop coupling, the assignment is [1$\underline{1}$2] for set I and [$\underline{1}$12] for set II. Only the collinear case matches the experimentally determined contrast, with set II being brighter in s- and slightly darker in p-geometry. Spin-flop coupling would produce the reverse contrast and can thus be excluded.

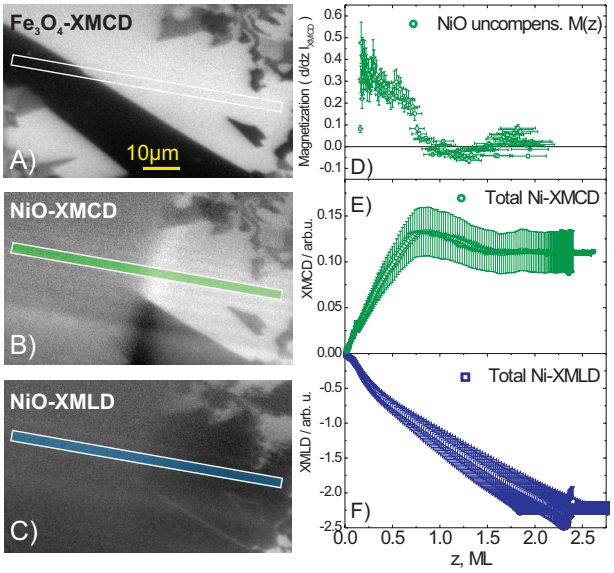

Fig. 3: (Color online) NiO wedge on Fe_3O_4. Left column: PEEM images with line profile position indicated. A) Fe XMCD (profile not shown), B) Ni-XMCD ratio image, C) NiO L_2 ratio image for s-polarized light. Right column: thickness-dependent line profile data: D) depth-profile of $M_{AF}(z)$ (derivative of total XMCD signal). E) Total Ni-XMCD signal *vs.* thickness. F) Total Ni-XMLD *vs.* thickness.

a single-crystalline material with O_h symmetry, the simple XMLD relation used in these previous analyses breaks down. It is valid only for orientation-averaged measurements, where any effects of the site symmetry will drop out. It has been shown recently that in oriented single-crystalline materials, the XMLD is *anisotropic*, *i.e.* depends on the spin orientation with respect to the crystal lattice [17,18]. We employ a model that is able to predict the XMLD angular variation for arbitrary spin orientations, allowing for a quantitative vectometry based on two fundamental spectra derived from atomic multiplet calculations.

The tiled center image (fig. 2) represents the local L_2 ratio in p- and s-contrast, which is related to both the orientation of the linear polarization **E** of the photon field and the orientation of the spin **S** with respect to the cubic crystal axes [18]. Our calculations (see contour plots in fig. 2) show best agreement with the experiment for a collinear coupling, *i.e.* the spin-axis of the AF is in-plane and oriented along [$\underline{1}$11] or [11$\underline{1}$]. At a first glance this seems to disagree with theory [19], since the NiO(110) interface should be fully compensated, if the bulk AF structure prevails at the interface. Our analyis will show that the Fe_3O_4/NiO *interface* is *not* compensated in the sense of Koon's theory, so the precondition for spin-flop coupling is actually not fulfilled.

Magnetic structure of the interface region. – We used XMCD at the Ni L edges to selectively study the magnetization in the adlayer (figs. 1 C and D). In order to prove that the NiO magnetization induced by the contact to the FIM is confined to the interface region, we compare two cases: a fractional 0.5 ML NiO coverage and a thick (35 ML) film. The resulting spectra are shown in fig. 1C. For 0.5 ML we get a maximum dichroic contrast of 54% in the white line. Both the magnitude and the spectral shape of the dichroism closely match the results of van der Laan (53%) for $NiFe_2O_4$ [20]. This means that the Ni moments are parallel to Fe_3O_4 and located at sites with octahedral oxygen coordination. From the spectra alone, $NiFe_2O_4$ and NiO cannot be distinguished, since Ni has the same oxygen coordination in both cases. As pointed out by Wang *et al.*, the NiO/Fe_3O_4 interface may in fact reconstruct to $NiFe_2O_4$, which is isostructural to Fe_3O_4 [9]. In the absence of thermal intermixing, this phase should be confined to one interfacial layer only. In contrast to the strong dichroism at 0.5 ML coverage we found a strongly reduced contrast of only 2.7% in the 35 ML film. Comparison of the intensity-normalized XMCD in both cases yields a rough estimate of 2.6 Å (1.7 ML) contributing to the XMCD signal. This low value thus indicates a good interface quality and has already been predicted for bilayers with ideal crystalline structure [2].

In order to determine the magnetic microstructure of the narrow proximity zone near the interface, a NiO stepped wedge was grown onto Fe_3O_4(110), with a step

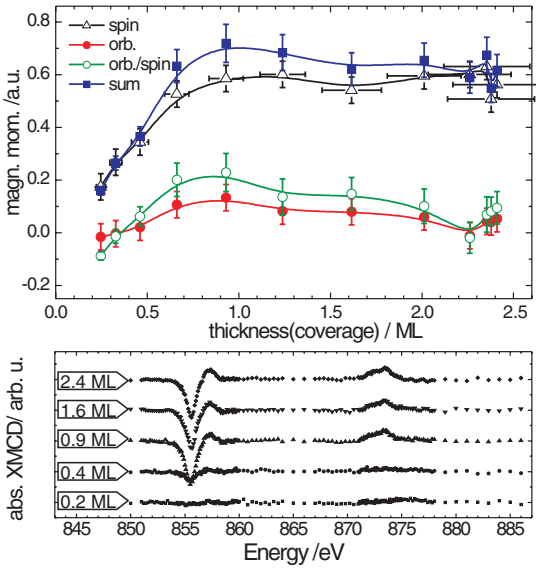

Fig. 4: (Color online) Local NiO-XMCD microspectra and sum rule analysis. The upper panel shows the thickness-dependent spin (open triangles) and orbital moments (circles), the ratio $m_{\mathrm{orb}}/m_{\mathrm{spin}}$ (open circles) and the sum $m_{\mathrm{orb}} + m_{\mathrm{spin}}$. (squares). The spin moment increases up to one monolayer and then stays constant for higher thicknesses, while the orbital moment shows a pronounced maximum near 1 ML and then decreases again. The origin of the minimum at 2.3 ML is still unclear. It could be caused by the completion of a second monolayer, but it could also be an artifact, since only a single data point is affected. Data points at higher thicknesses show a slightly increasing trend, but within the error margin their values are essentially the same as above 1 ML. Assuming an artifact, then m_{orb} is constant for thicknesses greater than 1.5 ML. The sum of orbital and spin moment closely resembles the curve already gained from the XMCD line profile, so the pronounced maximum near 1 ML is definitely caused by the orbital moment.

height of 2.5 ML (3.5 Å) and $\sim 20\,\mu$m wide step slopes. Since the interesting effects appear within the first few monolayers, we concentrate on the first step slope. In order to monitor the thickness-dependent changes in magnetic structure, we rely on the analysis of both image line profiles and microspectra. The line profiles were taken from PEEM parameter images, usually division images of two helicities (XMCD) or energies (XMLD), and provide a quick and convenient way to unravel the thickness-dependent changes in magnetic structure (see figs. 3A–C). The XMCD microspectra (fig. 4), in contrast, allow for a more detailed analysis with separation of spin and orbital contributions. In order to reduce intensity fluctuations, each XMCD spectrum was computed from a pair of areas of interest (AOI) belonging to a pair of 180° domains. The corresponding thickness calibration was done using the isotropic L_3 intensity, which at low thicknesses is proportional to the coverage. The latter was determined by quartz-balance evaporation rate measurements prior to and after deposition. In both the Ni-XMCD line profile

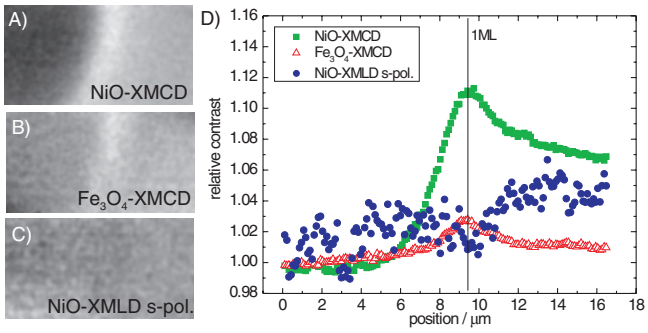

Fig. 5: (Color online) Enlargement of the slope area. Clearly, in all signals, an enhancement around one monolayer coverage can be observed, although in the Fe-XMCD and the Ni-XMLD the effect is only a few percent.

(fig. 3E) and the total magnetic moment (blue online squares in fig. 4), the same behaviour can be observed: The total moment increases up to a maximum, which is reached at a coverage near 1 ML. As soon as the second NiO monolayer starts to nucleate, the total moment decreases again and stays approximately constant above a thickness of ≈ 1.5 ML. In contrast to the XMCD, the XMLD signal increases (decreasing gray level) with a slight bend around 0.3 ML and approximately linear behaviour until it levels off at the step terrace.

The separation of m_{orb} and m_{spin} by a sum rule analysis shows that the extremum observed at one monolayer coverage is caused by the *orbital moment*, while the total spin moment increases until the first monolayer is completed. It then stays constant if further material is deposited on top (see fig. 4). This means that the NiO layer assumes its compensated antiferromagnetic structure already in the second monolayer, *i.e.* the uncompensated moments reside directly at the interface. Consequently, there is no planar domain wall forming in the ground state of the system, and the magnetic transition from ferri- to antiferromagnet is atomically sharp —in accordance with the findings from the electronic and structural transitions. This result is reasonable, since the magnetic interaction length is in the order of the lattice constant in poorly conducting correlated materials such as transition metal oxides.

In fig. 5, the slope region around one monolayer thickness is shown in more detail, now also including the Fe_3O_4-XMCD contrast profile. In all contrast patterns there is a clear extremum strictly confined to the thickness range around one monolayer. The peak in the Ni-XMCD as well as the coinciding dip in the Ni-XMLD indicate that an extremal value of the total magnetic moment magnitude $|\langle \boldsymbol{\mu} \rangle|$ and consequently also $|\langle \boldsymbol{\mu}^2 \rangle|$ must occur. The Fe_3O_4-XMCD contrast is enhanced by 3%, which corresponds —depending on the probing depth ($\lambda_e \approx 10$ Å [21] or $\lambda \approx 50$ Å [22])— to an enhancement of the total moment at the interface in the range of 120–200%. This increase could be caused by the Fe orbital moment —similar to Ni. On the other hand, it could also be a consequence of an electronic interaction between the Ni and Fe sites, for

example, if the interfacial monolayer reconstructs to $NiFe_2O_4$.

Note that Lueders *et al.* have found a considerable enhancement of the total magnetic moment up to 250% in ultrathin $NiFe_2O_4$ films [23]. If this effect is an intrinsic property of low-dimensional NFO, it could support the hypothesis of a $NiFe_2O_4$ interface layer. Provided that only one monolayer shows and enhanced Fe-XMCD signal, a 3% contrast enhancement with a probing depth of 50 Å would correspond to an enhancement as large as 200%, which comes close to the results in ref. [23].

Discussion of the results. – Since a bulk-truncated NiO(110) surface is atomically compensated, the occurence of collinear exchange coupling in our system is astonishing and at first glance contradicts the findings of Koon [19]. In the following, we will discuss possible reasons for the discrepancy. First, we have to consider the interface between the two materials Fe_3O_4 and NiO in more detail. If we compare the two structures, it becomes apparent that although magnetite has almost twice the crystallographic lattice constant of NiO, the *magnetic* unit cells of both materials match at the interface. This means that the two sublattices of NiO can experience different magnetic environments at the interface, leading to nondegenerate interface exchange constants $J_1 \neq J_2$. If the imbalance between these two coupling configurations is large enough, a spin-flop state is no longer stabilized and collinear coupling can occur. This is especially true, if we omit the somewhat idealized picture of bulk-truncated surfaces. Assuming for the moment that the interface layer reconstructs to $NiFe_2O_4$, Ni-cations will be located at octahedral positions only and the imbalance between J_1 and J_2 is enhanced.

These considerations are able to describe our findings for the (011)-interface. However, they have important implications for the coupling between the two materials in general, because this imbalance situation holds also for other surface orientations. Therefore, one would in fact expect collinear coupling for arbitrary interface orientations. In another study, however, we found spin-flop coupling for $Fe_3O_4(001)/NiO$ [24]. In general, the (001)-interface is atomically compensated and spin-flop coupling should therefore occur quite naturally, but the lifting of the NiO sublattice degeneracy by the inverse spinel structure of the magnetite discussed above should suppress this type of coupling. Thus, there must still be another mechanism at work, which introduces a dependence on the interface orientation. As will be discussed in the following, we believe that magnetoelastic effects —which have been neglected so far in most studies— play an important role in the magnetic coupling process.

Magnetoelastic effects, *e.g.* introduced by a lattice misfit, are well known to influence the magnetic behavior in ferromagnetic thin films. Similar effects must also be expected for antiferromagnets. Krishnakumar *et al.* [25] observed a thickness-dependent change in the magnetic anisotropy in Ag(001)/NiO, which they explained by strain relaxation, thereby involving magnetoelastic effects. Their hypothesis is supported by the finding that the presence of a MgO capping layer, which introduces additional strain, considerably weakened the thickness-dependent change in anisotropy. It should be noted in this context that Finazzi *et al.* have observed a similar transition from collinear to spin-flop coupling in Fe(001)/NiO at a critical AF thickness, but explained the effect by defects [26]. However, also in their case magnetoelastic effects might be of importance, since the lattice mismatch between the R45° NiO epitaxial growth and Fe is considerable (NiO is compressed in-plane by $\approx -3\%$). In our case of the (110)-surface, the lattice mismatch of NiO is considerably lower (in-plane tensile 0.5%). Nevertheless, we propose that magnetoelastic effects determine the coupling, and we will support this idea by qualitative arguments.

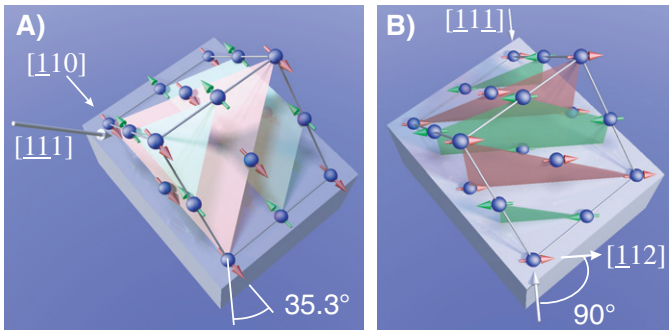

Fig. 6: (Color online) Two types of strain-induced AF stacking in $Fe_3O_4(110)/NiO$. A) the tensile in-plane epitaxial strain of NiO causes out-of-plane compression and stacking (for example along [111] as indicated in the figure). The intersection of the easy planes with the (110)-interface is the [1̄10]-direction. B) A hypothetical in-plane compression along one of the magnetite easy axes causes the spins of NiO to be perpendicular to magnetite, along the intersection of the easy planes and the interface. This case is never realized since the in-plane epitaxial strain is tensile, and moreover the magnetostriction in magnetite is positive along ⟨111⟩.

A single-domain NiO crystal shows a contraction by -0.15% along its ⟨111⟩-type stacking direction. Conversely, in a strained NiO layer those ⟨111⟩-directions, which are compressed most by the epitaxial strain, become favorable. For a $Fe_3O_4(110)/NiO$ interface this means that out-of-plane stacking should be favored over in-plane stacking (as in fig. 6A). If in-plane stacking were to occur (fig. 6B), the stacking vectors would be parallel to the in-plane easy directions ($[\pm 1 \mp 11]$) in magnetite, rendering the easy planes perpendicular to the interface. The intersecting in-plane easy directions of NiO would then be the $[\mp 1 \pm 12]$-directions, which in case of a stacking parallel to the Fe_3O_4 magnetization lead to spin-flop coupling (fig. 6B). All other configurations result in collinear coupling. Especially, since the actual stacking preferred by the epitaxial strain is out of plane, the easy directions of NiO are along [1̄10], and

thus closer to the magnetite easy axes (see fig. 6A). In this situation, collinear coupling is favoured, but the interfacial anisotropy will contain a uniaxial contribution along [1̄10]. In our as-grown samples, this contribution is not measurable, but becomes apparent, if we anneal the samples[1]. Finalizing our discussion, one could say that spin-flop coupling is "exotic" in our system, since it requires the right strain situation and/or a compensated interface. Both aspects are not realized and collinear coupling results naturally.

As a consequence of the above discussion, the coupling at the $Fe_3O_4(110)$/NiO interface should be seen as a delicate balance between at least two mechanisms: i) a competition between exchange coupling contributions from the FIM and AFM sublattices and ii) magnetoelastic interactions. As both mechanisms can independently lead to either collinear or spin-flop coupling, depending on the relative strength of the interactions, an *a priori* prediction of the coupling type for a given system is not trivial. This situation should also be encountered in many other exchange-bias systems, in particular, if a sizable lattice mismatch exists.

Summary and conclusions. – In summary, we found an enhanced Fe and Ni magnetization directly at the $NiO/Fe_3O_4(110)$ interface, which has its maximum at a coverage equivalent to 1 ML, implying a reconstruction of the interfacial monolayer towards the $NiFe_2O_4$ structure. Thus, the interface is not atomically compensated and collinear coupling can occur, in agreement with Koon's theory [19]. Another explanation for the collinear coupling lies in the epitaxially strained NiO layer, in which out-of-plane AF stacking vectors are preferred due to magnetoelastic effects. Sum rule analysis indicates that the extremum in the interfacial Fe and Ni total moments at one monolayer coverage might be caused by an enhanced orbital moment due to bonding anisotropy or an interaction of Ni and Fe cations in a NFO reconstructed interface layer. We found no evidence for a sign-reversal of the uncompensated magnetization in the antiferromagnet as postulated theoretically [2,7]. On the contrary, it appears that the electronic, magnetic and structural transition at the interface is atomically sharp and that already the second monolayer in the AF is fully compensated.

* * *

This work was partially funded by the Sonderforschungsbereich 491. We thank Y.-X. Su, D. Schrupp for supplying the synthetic magnetite crystals, M. Schmidt and C. Thomas for the Laue measurements. The authors dedicate this letter to the memory of Prof. F. U. Hillebrecht, a gifted scientist and good friend, who initiated this work.

[1]The influence of annealing on the magnetism in this material system exceeds the scope of the present paper and will be treated elsewhere.

REFERENCES

[1] Nogues J. and Schuller I. K., *J. Magn. & Magn. Mater.*, **192** (1999) 203.
[2] Jensen P. J., Dreyssé H. and Kiwi M., *Eur. J. Phys. B*, **46** (2005) 541.
[3] Fujii J., Borgatti F., Panaccione G., Hochstrasser M., Maccherozzi F., Rossi G. and van der Laan G., *Phys. Rev. B*, **73** (2006) 214444.
[4] Scholl A., Liberati M., Arenholz E., Ohldag H. and Stohr J., *Phys. Rev. Lett.*, **92** (2004) 247201.
[5] Qian X. and Hubner W., *Phys. Rev. B*, **67** (2003) 184414.
[6] Tyer R., van der Laan G., Temmerman W. M., Szotek Z. and Ebert H., *Phys. Rev. B*, **67** (2003) 104409.
[7] Finazzi M., *Phys. Rev. B*, **69** (2004) 064405.
[8] Recnik A., Carroll D. L., Shaw K. A., Lind D. M. and Ruhle M., *J. Mater. Res.*, **12** (1997) 2143.
[9] Wang H. Q., Gao W., Altman E. I. and Henrich V. E., *J. Vac. Sci. Technol. A*, **22** (2004) 1675.
[10] Regan T. J., Ohldag H., Stamm C., Nolting F., Luning J., Stohr J. and White R. L., *Phys. Rev. B*, **64** (2001) 214422.
[11] Tusche C., Meyerheim H. L., Hillebrecht F. U. and Kirschner J., *Phys. Rev. B*, **73** (2006) 125401.
[12] Ozdemir O., Xu S. and Dunlop D. J., *J. Geophys. Res.-Solid Earth*, **100** (1995) 2193.
[13] Haverkort M. W., Csiszar S. I., Hu Z., Altieri S., Tanaka A., Hsieh H. H., Lin H. J., Chen C. T., Hibma T. and Tjeng L. H., *Phys. Rev. B - Rapid Commun.*, **69** (2004) 020408(R).
[14] Alders D., Tjeng L. H., Voogt F. C., Hibma T., Sawatzky G. A., Chen C. T., Vogel J., Sacchi M. and Iacobucci S., *Phys. Rev. B*, **57** (1998) 11623.
[15] Hillebrecht F. U., Ohldag H., Weber N. B., Bethke C., Mick U., Weiss M. and Bahrdt J., *Phys. Rev. Lett.*, **86** (2001) 3419.
[16] Ohldag H., Scholl A., Nolting F., Anders S., Hillebrecht F. U. and Stohr J., *Phys. Rev. Lett.*, **86** (2001) 2878.
[17] Czekaj S., Nolting F., Heyderman L. J., Willmott P. R. and van der Laan G., *Phys. Rev. B - Rapid Commun.*, **73** (2006) 020401(R).
[18] Arenholz E., van der Laan G., Chopdekar R. V. and Suzuki Y., *Phys. Rev. B*, **74** (2006) 094407.
[19] Koon N. C., *Phys. Rev. Lett.*, **78** (1997) 4865.
[20] van der Laan G., Henderson C. M. B., Pattrick R. A. D., Dhesi S. S., Schofield P. F., Dudzik E. and Vaughan D. J., *Phys. Rev. B*, **59** (1999) 4314.
[21] Goering E., Gold S., Lafkioti M. and Schutz G., *Europhys. Lett.*, **73** (2006) 97.
[22] Gota S., Gautier-Soyer M. and Sacchi M., *Phys. Rev. B*, **62** (2000) 4187.
[23] Luders U., Bibes M., Bobo J. F., Cantoni M., Bertacco R. and Fontcuberta J., *Phys. Rev. B*, **71** (2005) 134419.
[24] Krug I. *et al.*, unpublished.
[25] Krishnakumar S., Liberati M., Grazioli C., Veronese M., Turchini S., Luches P. S. V. and Carbone C., *J. Magn. & Magn. Mater.*, **310** (2007) 8.
[26] Finazzi M., Brambilla A., Biagioni P., Graf J., Gweon G.-H., Scholl A., Lanzara A. and Duò L., *Phys. Rev. Lett.*, **97** (2006) 097202 .